



HAL
open science

Left ventricular torsion obtained using equilibrated warping in patients with repaired Tetralogy of Fallot

Daniel Alexander Castellanos, Kateřina Škardová, Abhijit Bhattaru, Ezgi Berberoglu, Gerald Greil, Animesh Tandon, Jeanne Dillenbeck, Barbara Burkhardt, Tarique Hussain, Martin Genet, et al.

► **To cite this version:**

Daniel Alexander Castellanos, Kateřina Škardová, Abhijit Bhattaru, Ezgi Berberoglu, Gerald Greil, et al.. Left ventricular torsion obtained using equilibrated warping in patients with repaired Tetralogy of Fallot. *Pediatric Cardiology*, 2021, 42 (6), pp.1275-1283. 10.1007/s00246-021-02608-y . hal-03204943

HAL Id: hal-03204943

<https://hal.science/hal-03204943>

Submitted on 22 Apr 2021

HAL is a multi-disciplinary open access archive for the deposit and dissemination of scientific research documents, whether they are published or not. The documents may come from teaching and research institutions in France or abroad, or from public or private research centers.

L'archive ouverte pluridisciplinaire **HAL**, est destinée au dépôt et à la diffusion de documents scientifiques de niveau recherche, publiés ou non, émanant des établissements d'enseignement et de recherche français ou étrangers, des laboratoires publics ou privés.

Title

Left ventricular torsion obtained using equilibrated warping in patients with repaired Tetralogy of Fallot

Authors

Daniel Alexander Castellanos MD¹
Kateřina Škardová MS²
Abhijit Bhattaru^{3,4}
Ezgi Berberoglu MS⁵⁻⁷
Gerald Greil MD PhD^{4,8}
Animesh Tandon MD^{4,8}
Jeanne Dillenbeck MD⁸
Barbara Burkhardt MD⁹
Tarique Hussain MD PhD^{4,8}
Martin Genet PhD^{6,7}
Radomir Chabiniok MD PhD^{2,4,6,7,10}

Institutions

¹Department of Cardiology, Boston Children's Hospital, Boston, MA, USA.

²Department of Mathematics, Faculty of Nuclear Sciences and Physical Engineering, Czech Technical University in Prague, Prague, CZ

³The College of New Jersey, Ewing, NJ, USA

⁴Division of Pediatric Cardiology, Department of Pediatrics, University of Texas Southwestern Medical Center, Dallas, TX, USA.

⁵Institute for Biomedical Engineering, Swiss Federal Institute of Technology, Zurich, Switzerland

⁶Solid Mechanics Laboratory (LMS), École Polytechnique / CNRS / Polytechnic Institute of Paris, France

⁷Inria, France

⁸Division of Pediatric Radiology, Department of Radiology, University of Texas Southwestern Medical Center, Dallas, TX, USA.

⁹Pediatric Heart Center, University Children's Hospital Zürich, Zürich, CH.

¹⁰School of Biomedical Engineering & Imaging Sciences (BMEIS), St Thomas' Hospital, King's College London, United Kingdom

Corresponding author:

Daniel Alexander Castellanos MD
300 Longwood Avenue, BCH 3215
Boston, MA 02115
Phone: 617-355-7275, Fax: 617-730-4791
Email: Daniel.castellanos@cardio.chboston.org

ORCID:

Daniel Alexander Castellanos MD: 0000-0003-1188-5257
Kateřina Škardová MS
Abhijit Bhattaru: 0000-0002-1383-1992
Ezgi Berberoglu MS
Gerald Greil MD PhD
Animesh Tandon MD: 0000-0001-9769-8801
Jeanne Dillenbeck MD
Barbara Burkhardt MD
Tarique Hussain MD PhD: 0000-0003-4091-992X
Martin Genet PhD: 0000-0003-2204-201X
Radomir Chabiniok MD PhD: 0000-0002-7527-2751

- 1 **Keywords:**
- 2 Tetralogy of Fallot
- 3 Early-stage heart failure
- 4 Motion tracking
- 5 Equilibrated warping
- 6 Torsion
- 7 Twist
- 8

1 Abstract**2 Purpose**

3 Patients after surgical repair of Tetralogy of Fallot (rTOF) may suffer a decrease in left ventricular (LV) function.
4 The aim of our study is to evaluate a novel method of assessing LV torsion in patients with rTOF, as an early
5 indicator of systolic LV dysfunction.

6 Methods

7 Motion tracking based on image registration regularized by the equilibrium gap principle, known as equilibrated
8 warping, was employed to assess LV torsion. Seventy-six cases of rTOF and ten normal controls were included. The
9 group of controls was assessed for reproducibility using both equilibrated warping and standard clinical tissue
10 tracking software (CVI42, version 5.10.1, Calgary, Canada). Patients were dichotomized into two groups: normal vs.
11 loss of torsion.

12 Results

13 Torsion by equilibrated warping was successfully obtained in 68 of 76 (89%) patients and 9 of 10 (90%) controls.
14 For equilibrated warping, the intra- and inter-observer coefficients of variation were 0.095 and 0.117, respectively;
15 compared to 0.260 and 0.831 for tissue tracking by standard clinical software. The intra- and inter-observer
16 intraclass correlation coefficients for equilibrated warping were 0.862 and 0.831, respectively; compared to 0.992
17 and 0.648 for tissue tracking. Loss of torsion was noted in 32 of the 68 (47%) patients with rTOF. There was no
18 difference in LV or RV volumes or ejection fraction between these groups.

19 Conclusion

20 The assessment of LV torsion by equilibrated warping is feasible and shows good reliability. Loss of torsion is
21 common in patients with rTOF and its robust assessment might contribute into uncovering heart failure in an earlier
22 stage.

23

1 **Declarations**

2
3 **Funding:** There was no specific funding source for this study. The study was partially supported by the Inria-UTSW
4 Associated Team TOFMOD. K. Škardová and R. Chabiniok were partially supported by project No. NV19-08-
5 00071 of the Ministry of Health of the Czech Republic.

6
7 **Conflicts of interest/Competing interests:** The authors report no conflict of interests.

8
9 **Ethics approval:** This study was approved by the University of Texas Southwestern Medical School Institutional
10 Review Board with a study ID of STU-2020-0023.

11
12 **Consent to participate:** The study was performed with a waiver of consent, as approved by the University of Texas
13 Southwestern Medical School Institutional Review Board with a study ID of STU-2020-0023. This is a retrospective
14 analysis of data collected in the normal medical care of patients. Transferring contact information to the principal
15 investigator and creating a consent document would pose a greater risk of loss of confidentiality to the participant
16 than the design of accessing a limited data set.

17
18 **Consent for publication:** The study was performed with a waiver of consent. This is a retrospective analysis of data
19 collected in the normal medical care of patients and does not include protect health information that can be used to
20 identify participants.

21
22 **Availability of data and material:** De-identified datasets are stored on password-protected servers within the
23 institution firewall. Data sharing agreements can be performed on a case-by-case basis.

24
25 **Code availability:** Software and tools to implement the equilibrated warping method of left ventricular torsion
26 assessment are freely available online, as described in the text and cited manuscripts.

27
28 **Authors' contributions:**

29 All authors approve the submitted version of the manuscript and have agreed to be personally accountable for their
30 contributions.

31
32 Daniel Alexander Castellanos made substantial contributions to the design of the work, analysis of data,
33 interpretation of data, and drafting of the manuscript.

34
35 Kateřina Škardová made substantial contributions to the analysis of data and creation of new software used in the
36 work.

37
38 Abhijit Bhattaru made substantial contributions to the acquisition of data, analysis of data, and interpretation of data.

39
40 Ezgi Berberoglu made substantial contributions to the analysis of data and creation of new software used in the
41 work.

42
43 Gerald Greil made substantial contributions to the acquisition of data and revision of the manuscript.

44
45 Animesh Tandon made substantial contributions to the acquisition of data and revision of the manuscript.

46
47 Jeanne Dillenbeck made substantial contributions to the acquisition of data and revision of the manuscript.

48
49 Barbara Burkhardt made substantial contributions through the acquisition of data, analysis of data, interpretation of
50 data, and revision of the manuscript.

51
52 Tarique Hussain made substantial contributions to the conception of the project, design of the work, acquisition of
53 data, analysis of data, interpretation of data, drafting of the manuscript, and revision of the manuscript.

54
55 Martin Genet made substantial contributions to the design of the work, interpretation of data, revision of the
56 manuscript, and creation of new software used in the work.

- 1
- 2 Radomir Chabiniok made substantial contributions to the design of the work, interpretation of data, revision of the
- 3 manuscript, and creation of new software used in the work.
- 4

1 **Introduction**

2 Patients after surgical repair of Tetralogy of Fallot (rTOF) tend to have suboptimal left ventricular mechanics and
3 may suffer a loss in left ventricular function [1–7]. Ventricular dysfunction has been associated with poor clinical
4 outcomes, including death [1, 3–5]. There is literature to support the notion that pulmonary regurgitation and
5 impaired right ventricular function result in impaired left ventricular mechanics [8]. Such findings would suggest
6 that there is an insidious progression of left ventricular dysfunction beginning in childhood. Parameters that assess
7 left ventricular mechanics have been associated with greater risk of sudden cardiac death [9]. Therefore, early
8 identification of deteriorating left ventricular mechanics and function may guide clinical management in this
9 population.

10

11 Torsion, also known as twist, is a characteristic feature of the ventricular contraction [10]. It is often reported as the
12 maximal net difference in rotation between the LV apex and base at peak systole [11–17] and is expressed in
13 degrees. When divided by the distance between base and apex, the LV twist gradient (expressed in degrees per
14 centimeter) is obtained to adjust for differences in LV dimensions between patients [13, 16]. In comparison to
15 ventricular ejection fraction (a global indicator of ventricular systolic function) LV torsion is rarely reported in the
16 clinic. However, it has the potential to detect the deterioration of cardiac function in earlier stages [10]. This
17 substantiates the assessment of LV torsion in cardiac patients, both with acquired and congenital heart disease. In
18 particular for the patients with repaired Tetralogy of Fallot, studies suggest that adverse ventricular-ventricular
19 interactions may result in reduced LV torsion [12, 15, 16]. However, tissue tracking analysis performed in standard
20 clinical software to calculate left ventricular torsion in this population have documented poor intraobserver and
21 interobserver reliability, with high coefficient of variation and low intraclass correlation coefficient [13].

22

23 Image registration is the process of aligning two or more images. It can be used to extract the motion of moving
24 structures in images, such as the motion of the left ventricle from cine sequences in cardiac MRI. Features of
25 interest, such as the evolution of torsion over time, can be obtained by the analysis of extracted motion. The aim of
26 our study is to evaluate a novel motion tracking method based on image registration regularized by biomechanical
27 properties of myocardium, named *equilibrated warping* [18, 19]. Equilibrated warping is based on the finite element
28 method for image registration and the mechanical equilibrium principle for regularization. Specifically, the image

1 intensity of points on the LV myocardium on cine sequences is used as the similarity metric to track trajectories
2 between frames. At the same time, the deformation of the myocardium (represented by a finite element mesh) is
3 constrained by the so-called finite strain equilibrium gap [18–20]. The intrinsic biomechanical tissue properties,
4 represented by the rigidity (stiffness) of the hyperelastic model, prevents the LV myocardium from unphysiological
5 deformations during the tracking of points within myocardial tissue.

6

7 This study aims to use equilibrated warping to assess LV torsion in patients with rTOF and explore the relationship
8 between LV torsion and other cardiac parameters obtained on routine cardiac MRI. We hypothesize that equilibrated
9 warping will reliably obtain ventricular torsion and that the decrease or reversing of torsion will be associated with
10 increased right ventricular end-diastolic volume, decreased right ejection fraction, and decreased left ventricular
11 ejection fraction.

12

13 **Materials and Methods**

14 This was a single center retrospective study using anonymized data obtained from routine clinical scans. Seventy-six
15 cases of repaired Tetralogy of Fallot and ten normal controls were included. Ventricular contours were manually
16 segmented as a part of routine clinical work (**Figure 1**) by using standard clinical software (CVI42, version 5.10.1,
17 Calgary, Canada). RV end-systolic volume (RVESV), RV end-diastolic volume (RVEDV), RV ejection fraction
18 (RVEF), LVESV, LVEDV, LVEF were then exported for each subject. Additionally, end-diastolic LV endocardial
19 and epicardial surfaces, generated from the manually segmented contours in CVI42, were saved as STL surface
20 meshes using the export function built in the CVI42 software. The surface meshes and the short-axis cine MR
21 images served as input into the equilibrated warping workflow (described below) to obtain the LV peak systolic
22 twist (torsion) and peak systolic twist gradient (normalized by mesh length).

23

24 The equilibrated warping method was implemented using the FEniCS (open source finite element library) and VTK
25 (open source library for mesh and image manipulation) libraries, and are distributed as a freely available Python
26 library [20]. The workflow of applying the equilibrated warping to our problem is depicted in **Figure 2**, where most
27 steps have been automatized through a custom script. The inputs are ventricular short-axis cine images (in DICOM

1 format) and the end-diastolic LV endocardial and epicardial surface meshes (in STL format). Then, MeVisLab (an
2 application framework for medical image processing and visualization, version 3.0.2, Bremen, Germany) was used
3 to resample the DICOM images to an isotropic voxel size. The LV endocardial and epicardial surface meshes are
4 then used to generate a volume mesh of LV myocardium by using GMSH (a free three-dimensional finite element
5 mesh generator, version 3.0.6, Belgium). First, the endocardial and epicardial surfaces are re-meshed by GMSH,
6 such that they are made of well-shaped (i.e, close to equilateral) triangles, which is required for finite element
7 computations [21]. Then, a volume mesh of LV myocardium is created by using first order tetrahedra finite elements
8 [22]. The volume mesh is then divided into ten equally spaced longitudinal (base to apex) sectors with the center of
9 mass for each sector defined along the left ventricular axis. **Figure 3** demonstrates the final volume mesh overlaid
10 on cine images of a selected patient. This mesh is then used for the torsion analysis. Equilibrated warping was then
11 employed throughout the cardiac cycle to track tissue motion within the LV myocardium encompassed by the
12 volume mesh in the short axis cine images and morph the end-diastolic volume mesh (**Figure 2**). ParaView
13 visualization software (version 5.7.0, Clifton Park, NY, USA) was used as an intermediary for viewing and quality
14 check of the meshes. The torsion of each of the mesh points was computed from the deforming volume meshes.
15 Finally, the peak twist gradient was defined as the systolic basal rotation minus systolic apical rotation, normalized
16 by the ventricular length.

17

18 The cases analyzed by equilibrated warping that did not have enough signal to determine torsion were excluded
19 from the final analysis (as defined by an unacceptably high standard deviation of rotation values with visually
20 uninterpretable rotation curves). The patients with rTOF in which torsion was successfully analyzed were
21 dichotomized into two groups by visual inspection of torsion over the cardiac cycle: those with normal systolic
22 torsion (systolic basal clockwise rotation and apical counterclockwise rotation) and those with loss of systolic
23 torsion, defined as a loss of normal systolic basal clockwise rotation. In the group of normal controls, torsion was
24 calculated by equilibrated warping and standard tissue tracking software (using CVI42). Intra- and interobserver
25 variability for both methods of torsion was calculated among patients in the control group. The comparison between
26 normal and abnormal torsion was performed only among patients with repaired TOF.

27

1 Ventricular volumes were indexed to body surface area. Statistical analyses were performed with IBM SPSS
2 Statistics 25 (IBM Corporation, Armonk, NY, USA). Continuous data are expressed as mean \pm SD or as median
3 (range) as appropriate. The Shapiro-Wilk test was used to assess for normal distribution. Coefficients of variation
4 (SDs of differences between two measurements, divided by the respective means of two measurements) and
5 intraclass correlation coefficients were calculated to describe intra- and interobserver variability of torsion obtained
6 in the control group by both the tissue tracking analysis in standard clinical software (CVI42) and using equilibrated
7 warping. In the patients with repaired TOF, ventricular parameters for the groups with and without normal torsion
8 were compared by Mann-Whitney U tests for non-normally distributed variables and independent sample t-test for
9 normally distributed variables. This study was approved by the University of Texas Southwestern Medical School
10 Institutional Review Board.

11

12 **Results**

13 Torsion by equilibrated warping was successfully obtained in 68 of 76 (89%) patients with repaired TOF and 9 of 10
14 (90%) normal controls. A representative example of normal torsion is shown in **Figure 4** and a representative
15 example of loss of torsion is shown in **Figure 5**.

16

17 The median age of control patients was 23 years (range of 9 years to 30 years). For equilibrated warping, the intra-
18 and inter-observer coefficients of variation were 0.095 and 0.117, respectively; compared to 0.260 and 0.831 for
19 tissue tracking by standard clinical software. The intra- and inter-observer intraclass correlation coefficients for
20 equilibrated warping were 0.862 and 0.831, respectively; compared to 0.992 and 0.648 for tissue tracking.

21

22 Loss of systolic torsion was noted in 32 of the 68 (47%) patients with repaired TOF (**Table 1**). Patients with loss of
23 torsion tended to be younger at the time of MRI. There was a significant difference in peak systolic twist gradient
24 between patients with normal torsion and loss of torsion. There was no difference in RVESV, RVEDV, RVEF,
25 LVESV, LVEDV, and LVEF between the groups.

26

27 The patients with repaired TOF in whom equilibrated warping was not successful, were on average 11.9 years of age
28 and were 9.8 years from their last pulmonary valve intervention (**Table 2**). Aside from right ventricular dilation, no

1 other significant abnormalities were noted on ventricular parameters at cardiac MRI. The average right ventricular
2 dilation was lower than in the patients with rTOF for whom the motion tracking by equilibrated warping was
3 successful.

4

5 **Discussion**

6 Motion tracking by equilibrated warping can be used to extract features of left ventricular deformation. It has been
7 shown to be able to predict global torsion in cine images as well in 3D tagged or 3D echocardiography images,
8 despite low contrast [18, 19]. In present work we applied the equilibrated warping to assess the LV torsion in
9 patients with repaired Tetralogy of Fallot with a 90% success rate. LV torsion is known to be affected at an early
10 stage in several cardiac diseases. The median age of patients with rTOF in whom we observed the loss of systolic
11 LV torsion, was 11.7 years. This could correspond to an early sign of functional deterioration of their left ventricle.
12 The equilibrated warping method of motion tracking may serve as a valuable tool by producing a robust non-
13 invasive marker for left ventricular mechanics in patients who may suffer insidious progression of left ventricular
14 dysfunction beginning in childhood.

15

16 There was no significant association between the loss of torsion and other ventricular parameters indicative of a
17 worsening cardiac condition, such as increased right ventricular end-diastolic volume or a decreased ventricular
18 ejection fraction. Long-term follow-up of this population is necessary to assess the relationship of loss of left
19 ventricular torsion with worsening ventricular parameters and other poor clinical outcomes.

20

21 We advocate that visual inspection of the graphical output of torsion over time is a necessary step in analyzing
22 torsion. While the peak systolic twist gradient was lower in patients who were visually determined to have poor
23 torsion, there are cases where the peak systolic twist gradient alone may not convey impaired left ventricular
24 mechanics. For instance, cases in which there is loss of basal torsion and intact apical torsion may have a reasonable
25 twist gradient (reference **Figure 5**). As loss of basal torsion implies impaired left ventricular mechanics, we included
26 these cases in the loss of torsion group along with patients who had a loss of both basal and apical torsion and a
27 resultant low peak systolic twist gradient.

28

1 On the present study we showed a good intraobserver intraclass correlation coefficient using the standard tissue
2 tracking method albeit with unacceptably low interobserver intraclass correlation coefficient. This is, however, more
3 testament to the fact that using the intraclass correlation coefficient alone is an imperfect way of showing agreement
4 [22]. Our data does continue to show too high a coefficient of variance, suggesting poor overall interobserver and
5 intraobserver agreement. This agrees with our previous work on this subject [12].
6

7 There are limitations in the equilibrated warping method workflow. First, it requires the creation of LV volume
8 mesh out of the LV endocardium and epicardium surface meshes (exported from CVI42). This technical step was
9 not fully automatized in present study and caused an increased time of post-processing and a more complex learning
10 curve relative to other methods. Further automation (such as full automation of volume mesh creation from the
11 segmented endo- and epicardial contours, reference **Figure 2**) will alleviate this issue and is a future step for the
12 authors to translate this method into routine clinical practice.
13

14 As evidenced by the 8 patients with rTOF (**Table 2**) and 1 normal control subject in whom the motion tracking by
15 equilibrated warping failed, there are still issues with this motion tracking method. There was no clear anatomic or
16 functional difference between these patients and the ones in which torsion by equilibrated warping was successful.
17 These errors may be a result of interpolating short-axis cine stacks in the longitudinal direction. One possible
18 solution to this is combining short-axis cine stacks with another series of images (such as long-axis cine slices).
19 Secondly, the image similarity metrics to extract the motion in this work was simply based on the image intensity.
20 Other metrics could be used as well, such as including a distance between contours [23] or involving a model of the
21 imaging process [24]. Such components have the potential to improve the motion tracking and their implementation
22 and assessment is our ongoing work.
23

24 Overall, the motion tracking by equilibrated warping to estimate the LV torsion is feasible in patients with rTOF and
25 shows good reliability. The input requires only the ventricular short axis cine DICOMS and the end-diastolic
26 contours already segmented during routine clinical work. Therefore, the present workflow of advanced image
27 processing could be used in addition to the standard clinical analysis (measurement of ventricular volumes) without

1 repeating the contouring of the endocardial and epicardial surfaces. This would prevent a possible error caused by
2 re-contouring and has the advantage of no additional time for image segmentation.

3

4 Tracking motion in tagged MR images, either by image registration based methods such as equilibrated warping
5 [18] or by methods specific to a tagged pattern such as Harmonic Phase analysis (HARP) [25–27] or sine-wave
6 modelling [28], would be likely to increase the accuracy of LV torsion. While it is unlikely that analyzing tagged
7 MRI would change the global classification of patients (with torsion vs. with loss of torsion), it might lead to a
8 reduction of subjects in whom our workflow failed. While it is out of scope of the present work, in the future we
9 intend to recruit a group of patients for whom short-axis stacks of cine and tagged MRI will be acquired and the
10 torsion analyzed by the two methods.

11

12 Our pilot study shows that loss of torsion is common in patients with rTOF. Additionally, there was no significant
13 association between the loss of torsion and other ventricular parameters indicative of a worsening cardiac condition.
14 Future studies committed to the long-term follow-up of this population are needed to assess the role of torsion in
15 predicting ventricular dysfunction and death. Finally, while this study is performed on a cohort of patients with
16 rTOF, the results could also apply to the assessment of torsion in other cardiac patients. The fundamental principle
17 of our method, incorporating known physiologic and biophysical properties into image processing techniques, has
18 the potential to improve image analysis such that it contributes to an earlier identification of derangements in cardiac
19 function [29, 30]. Such an advancement may eventually result in an earlier institution of therapies that prevent a late
20 deterioration in myocardial function.

21

1 References

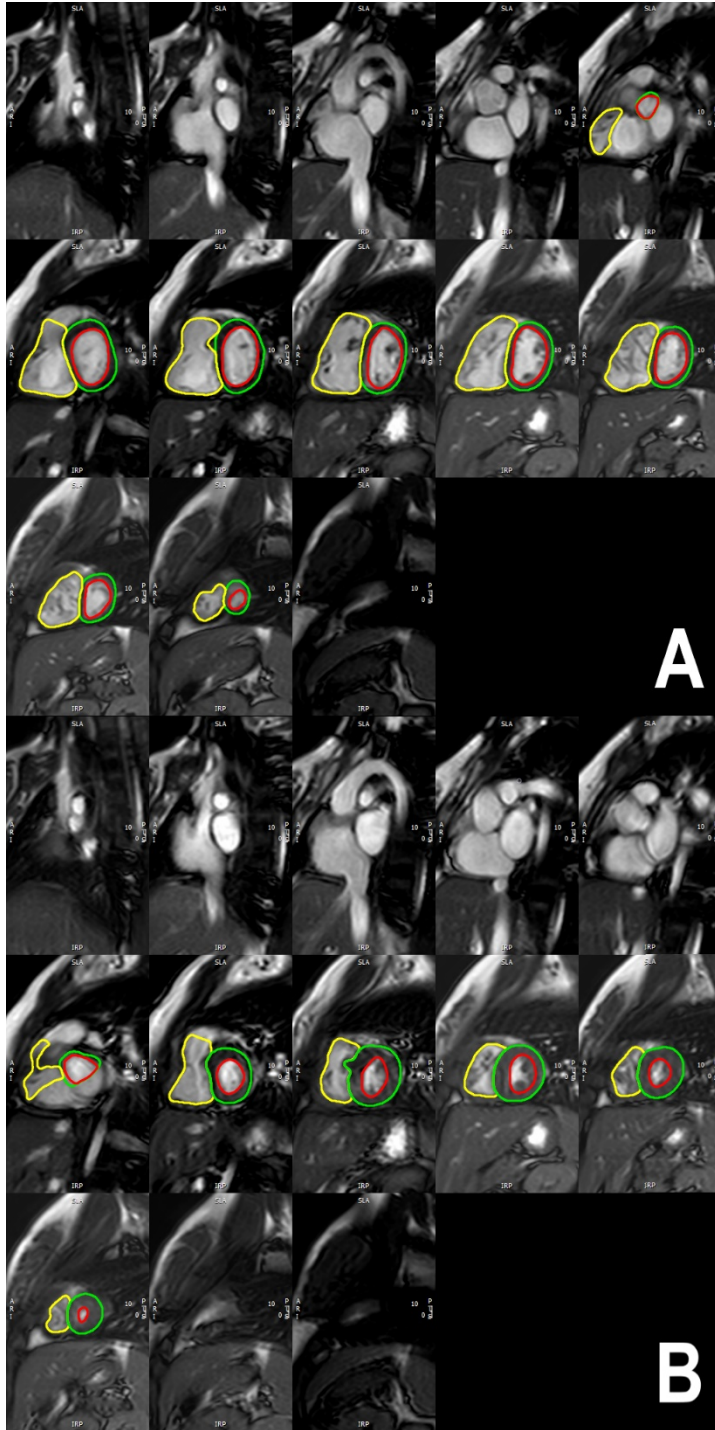
- 2 1. Geva T, Sandweiss BM, Gauvreau K, et al (2004) Factors associated with impaired clinical status in long-term
3 survivors of tetralogy of Fallot repair evaluated by magnetic resonance imaging. *J Am Coll Cardiol* 43:1068–
4 1074. <https://doi.org/10.1016/j.jacc.2003.10.045>
- 5 2. Tzemos N, Harris L, Carasso S, et al (2009) Adverse left ventricular mechanics in adults with repaired tetralogy
6 of Fallot. *Am J Cardiol* 103:420–425. <https://doi.org/10.1016/j.amjcard.2008.09.101>
- 7 3. Valente AM, Gauvreau K, Assenza GE, et al (2014) Contemporary predictors of death and sustained ventricular
8 tachycardia in patients with repaired tetralogy of Fallot enrolled in the INDICATOR cohort. *Heart* 100:247–
9 253. <https://doi.org/10.1136/heartjnl-2013-304958>
- 10 4. Ghai A, Silversides C, Harris L, et al (2002) Left ventricular dysfunction is a risk factor for sudden cardiac
11 death in adults late after repair of tetralogy of Fallot. *J Am Coll Cardiol* 40:1675–1680.
12 [https://doi.org/10.1016/s0735-1097\(02\)02344-6](https://doi.org/10.1016/s0735-1097(02)02344-6)
- 13 5. Knauth AL, Gauvreau K, Powell AJ, et al (2008) Ventricular size and function assessed by cardiac MRI predict
14 major adverse clinical outcomes late after tetralogy of Fallot repair. *Heart* 94:211–216.
15 <https://doi.org/10.1136/hrt.2006.104745>
- 16 6. Friedberg MK, Fernandes FP, Roche SL, et al (2012) Impaired right and left ventricular diastolic myocardial
17 mechanics and filling in asymptomatic children and adolescents after repair of tetralogy of Fallot. *Eur Heart J*
18 *Cardiovasc Imaging* 13:905–913. <https://doi.org/10.1093/ehjci/jes067>
- 19 7. Davlouros PA, Kilner PJ, Hornung TS, et al (2002) Right ventricular function in adults with repaired tetralogy
20 of Fallot assessed with cardiovascular magnetic resonance imaging: detrimental role of right ventricular
21 outflow aneurysms or akinesia and adverse right-to-left ventricular interaction. *J Am Coll Cardiol* 40:2044–
22 2052. [https://doi.org/10.1016/s0735-1097\(02\)02566-4](https://doi.org/10.1016/s0735-1097(02)02566-4)
- 23 8. Fernandes FP, Manlhiot C, Roche SL, et al (2012) Impaired left ventricular myocardial mechanics and their
24 relation to pulmonary regurgitation, right ventricular enlargement and exercise capacity in asymptomatic
25 children after repair of tetralogy of Fallot. *J Am Soc Echocardiogr* 25:494–503.
26 <https://doi.org/10.1016/j.echo.2012.01.014>
- 27 9. Diller G-P, Kempny A, Liodakis E, et al (2012) Left ventricular longitudinal function predicts life-threatening
28 ventricular arrhythmia and death in adults with repaired tetralogy of fallot. *Circulation* 125:2440–2446.
29 <https://doi.org/10.1161/CIRCULATIONAHA.111.086983>
- 30 10. Sengupta PP, Tajik AJ, Chandrasekaran K, Khandheria BK (2008) Twist mechanics of the left ventricle:
31 principles and application. *JACC Cardiovasc Imaging* 1:366–376. <https://doi.org/10.1016/j.jcmg.2008.02.006>
- 32 11. Chang M-C, Wu M-T, Weng K-P, et al (2018) Left ventricular regional myocardial motion and twist function
33 in repaired tetralogy of Fallot evaluated by magnetic resonance tissue phase mapping. *Eur Radiol* 28:104–114.
34 <https://doi.org/10.1007/s00330-017-4908-7>
- 35 12. van der Hulst AE, Delgado V, Holman ER, et al (2010) Relation of left ventricular twist and global strain with
36 right ventricular dysfunction in patients after operative “correction” of tetralogy of fallot. *Am J Cardiol*
37 106:723–729. <https://doi.org/10.1016/j.amjcard.2010.04.032>
- 38 13. Burkhardt BEU, Velasco Forte MN, Durairaj S, et al (2017) Timely Pulmonary Valve Replacement May Allow
39 Preservation of Left Ventricular Circumferential Strain in Patients with Tetralogy of Fallot. *Front Pediatr* 5:39.
40 <https://doi.org/10.3389/fped.2017.00039>

- 1 14. Karnik R, Uppu SC, Tozzi M, et al (2018) Abnormalities in Left Ventricular Rotation Are Inherent in Young
2 Children with Repaired Tetralogy of Fallot and Are Independent of Right Ventricular Dilation. *Pediatr Cardiol*
3 39:1172–1180. <https://doi.org/10.1007/s00246-018-1877-9>
- 4 15. Dragulescu A, Friedberg MK, Grosse-Wortmann L, et al (2014) Effect of chronic right ventricular volume
5 overload on ventricular interaction in patients after tetralogy of Fallot repair. *J Am Soc Echocardiogr* 27:896–
6 902. <https://doi.org/10.1016/j.echo.2014.04.012>
- 7 16. Li S-N, Yu W, Lai CT-M, et al (2013) Left ventricular mechanics in repaired tetralogy of Fallot with and
8 without pulmonary valve replacement: analysis by three-dimensional speckle tracking echocardiography. *PLoS*
9 *ONE* 8:e78826. <https://doi.org/10.1371/journal.pone.0078826>
- 10 17. Menting ME, Eindhoven JA, van den Bosch AE, et al (2014) Abnormal left ventricular rotation and twist in
11 adult patients with corrected tetralogy of Fallot. *Eur Heart J Cardiovasc Imaging* 15:566–574.
12 <https://doi.org/10.1093/ehjci/jet244>
- 13 18. Genet M, Stoeck CT, von Deuster C, et al (2018) Equilibrated warping: Finite element image registration with
14 finite strain equilibrium gap regularization. *Med Image Anal* 50:1–22.
15 <https://doi.org/10.1016/j.media.2018.07.007>
- 16 19. Lee LC, Genet M (2019) Validation of Equilibrated Warping—Image Registration with Mechanical
17 Regularization—On 3D Ultrasound Images. In: Coudière Y, Ozenne V, Vigmond E, Zenzemi N (eds)
18 *Functional Imaging and Modeling of the Heart: FIMH 2019*. Springer, Cham, Switzerland, pp 334–341
- 19 20. Genet M GENET Martin / dolfin_dic. In: GitLab at INRIA. https://gitlab.inria.fr/mgenet/dolfin_dic. Accessed
20 10 Sep 2019
- 21 21. Remacle J-F, Geuzaine C, Compère G, Marchandise E (2010) High-quality surface remeshing using harmonic
22 maps. *International Journal for Numerical Methods in Engineering* 83:403–425.
23 <https://doi.org/10.1002/nme.2824>
- 24 22. Geuzaine C, Remacle J-F (2009) Gmsh: a three-dimensional finite element mesh generator with built-in pre-
25 and post-processing facilities. *Int J Numer Meth Engng* 79:1309–1331
- 26 23. Škardová K, Oberhuber T, Tintěra J, Chabiniok R (2020) Signed-distance function based non-rigid registration
27 of image series with varying image intensity. *Discrete & Continuous Dynamical Systems - S* 13:.
28 <https://doi.org/doi:10.3934/dcdss.2020386>
- 29 24. Škardová K, Rambašek M, Chabiniok R, Genet M (2019) Mechanical and Imaging Models-Based Image
30 Registration. In: Tavares JMRS, Natal Jorge RM (eds) *VipIMAGE 2019*. Springer International Publishing,
31 Cham, pp 77–85
- 32 25. Osman NF, Kerwin WS, McVeigh ER, Prince JL (1999) Cardiac motion tracking using CINE harmonic phase
33 (HARP) magnetic resonance imaging. *Magn Reson Med* 42:1048–1060. [https://doi.org/10.1002/\(sici\)1522-
34 2594\(199912\)42:6<1048::aid-mrm9>3.0.co;2-m](https://doi.org/10.1002/(sici)1522-2594(199912)42:6<1048::aid-mrm9>3.0.co;2-m)
- 35 26. Osman NF, McVeigh ER, Prince JL (2000) Imaging heart motion using harmonic phase MRI. *IEEE Trans Med*
36 *Imaging* 19:186–202. <https://doi.org/10.1109/42.845177>
- 37 27. Mella H, Mura J, Wang H, et al (2021) HARP-I: A Harmonic Phase Interpolation Method for the Estimation of
38 Motion from Tagged MR Images. *IEEE Trans Med Imaging PP*: <https://doi.org/10.1109/TMI.2021.3051092>
- 39 28. Arts T, Prinzen FW, Delhaas T, et al (2010) Mapping displacement and deformation of the heart with local
40 sine-wave modeling. *IEEE Trans Med Imaging* 29:1114–1123. <https://doi.org/10.1109/TMI.2009.2037955>

- 1 29. Wong J, Chabiniok R, Tibby SM, et al (2018) Exploring kinetic energy as a new marker of cardiac function in
2 the single ventricle circulation. *J Appl Physiol* (1985) 125:889–900.
3 <https://doi.org/10.1152/jappphysiol.00580.2017>

- 4 30. Ruijsink B, Zugaj K, Wong J, et al (2020) Dobutamine stress testing in patients with Fontan circulation
5 augmented by biomechanical modeling. *PLoS ONE* 15:e0229015.
6 <https://doi.org/10.1371/journal.pone.0229015>

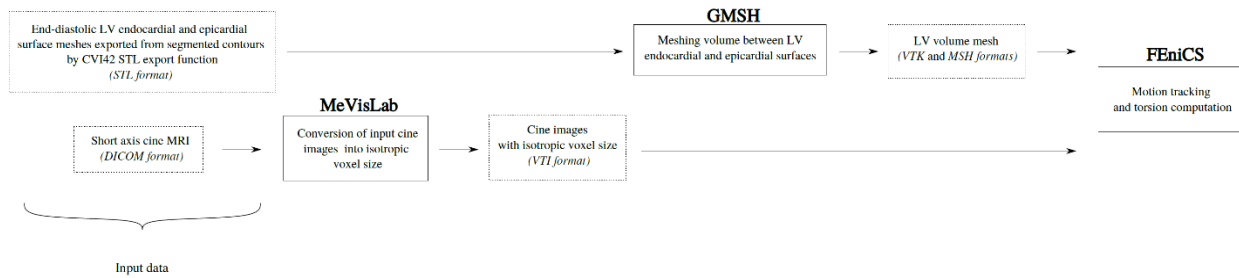
7



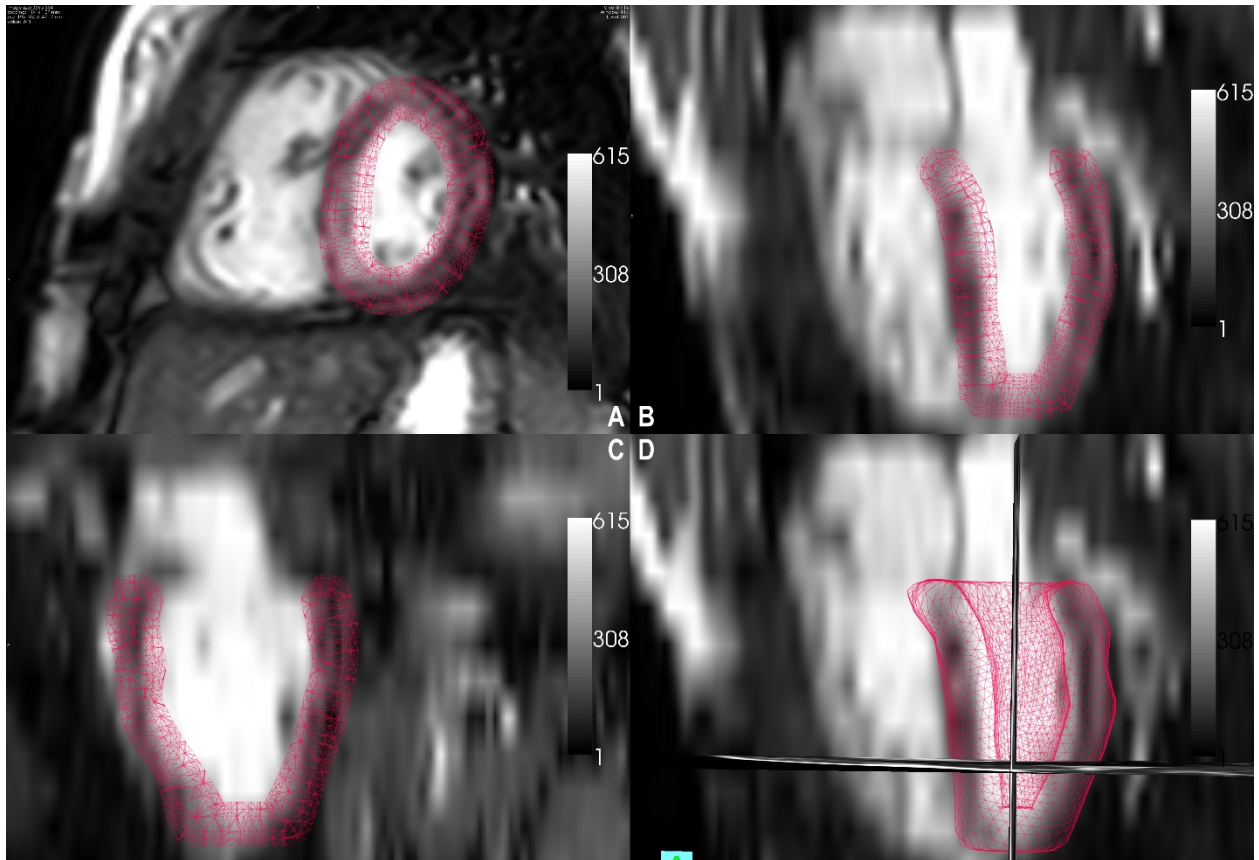
1

2 **Figure 1:** Ventricular contours were manually segmented as a part of routine clinical work. An example of
 3 ventricular contours in a patient with repaired Tetralogy of Fallot is shown. Panel A demonstrates contours during
 4 ventricular diastole. Panel B demonstrates contours during ventricular systole.

5

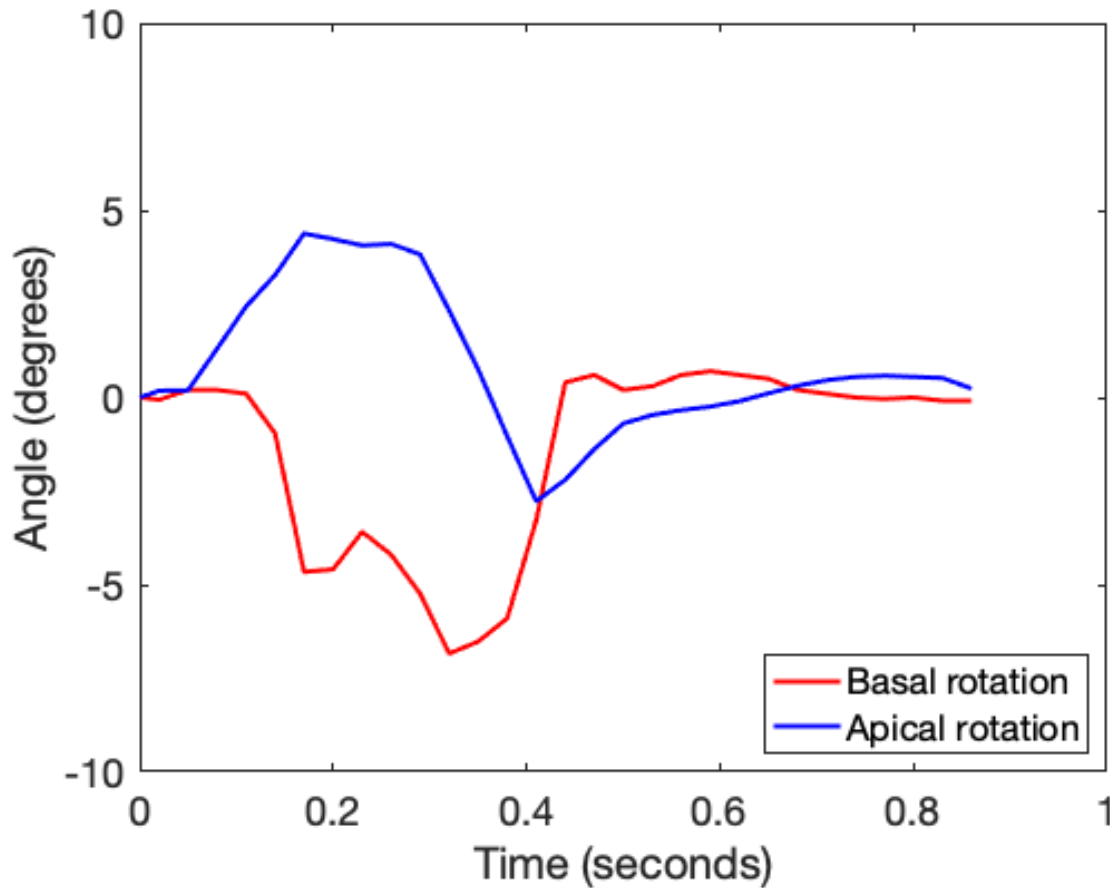


1
2 **Figure 2:** Workflow used during this study to calculate ventricular torsion using the equilibrated warping method.
3 The inputs are ventricular short axis cine DICOMS and the end-diastolic contours segmented during routine clinical
4 work. MeVisLab (version 3.0.2, Bremen, Germany) is an application framework for medical image processing and
5 visualization. GMSH (version 3.0.6, Belgium) is a three-dimensional finite element mesh generator. ParaView
6 (version 5.7.0, Clifton Park, NY, USA) was used as an intermediary. The tools are freely available.
7

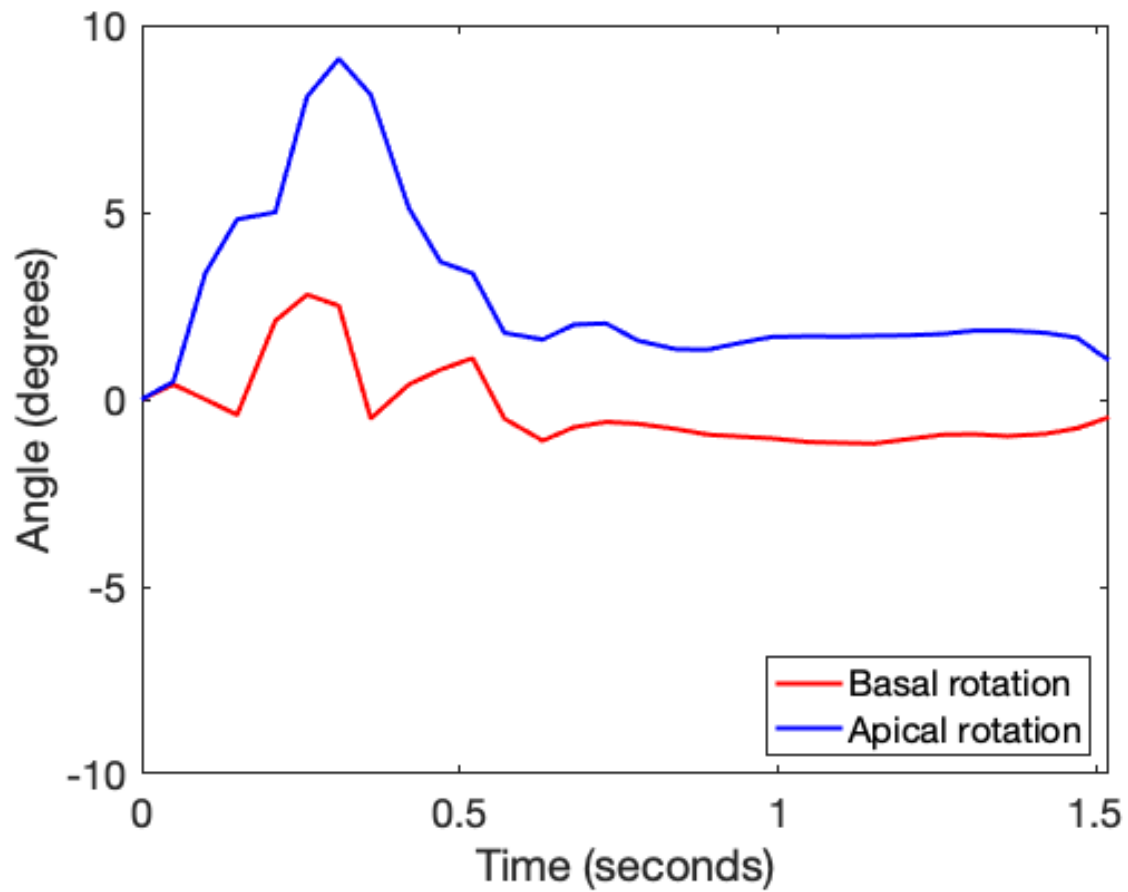


1

2 **Figure 3:** As part of the workflow for equilibrated warping, a volume mesh of the left ventricular myocardium is
 3 generated from the clinical contours of the ventricular short axis cines. A: The mesh is overlaid on a mid-
 4 ventricular slice of the short axis cine. B and C: The mesh is overlaid on long-axis images that were reconstructed
 5 from the short axis cine. D: A 3-D representation of the mesh is shown on a reconstructed long-axis image.



1
2 **Figure 4:** Normal torsion in a patient with repaired Tetralogy of Fallot. The x-axis represents time (seconds) during
3 the cardiac cycle and the y-axis represents torsion (degrees). During systole, the base undergoes clockwise rotation
4 (negative y-axis values) while the apex undergoes counterclockwise rotation (positive y-axis values). Peak systolic
5 twist is 9.16 degrees and occurs at 0.32 seconds. When normalized to mesh length, the peak systolic twist gradient is
6 0.12 degrees/cm.
7
8



1
 2 **Figure 5:** Reversal of normal basal systolic rotation in a patient with repaired Tetralogy of Fallot. During systole,
 3 both the base and apex undergo counterclockwise rotation. Peak systolic twist is 8.65 degrees and occurs at 0.36
 4 seconds. When normalized to mesh length, the peak systolic twist gradient is 0.10 degrees/cm.
 5

Variable	Normal torsion (n=36)	Abnormal torsion (n=32)	P-value
Patients with shunt prior to initial repair	5 (13.9%)	4 (12.5%)	1.000
Age at MRI (years)	16.2 (1.9-39.6)	11.7 (3.4, 52.1)	0.012
Time from pulmonary valve intervention to MRI (years)	13.2 (0.7-37.6)	9.9 (2.9-49.6)	0.353
Peak systolic twist (degrees)	10.19 (3.82-23.60)	6.42 (1.71-17.19)	<0.001
Peak systolic twist gradient (degrees/cm)	0.16 (0.06-0.35)	0.01 (-0.08-0.28)	<0.001
RVEDVi (ml/m ²)	135 +/- 36	134 +/- 37	0.880
RVESVi (ml/m ²)	66 (37-121)	68 (27-125)	0.731
RVEF (%)	47.6 +/- 6.8	49.2 +/- 8.3	0.367
LVEDVi (ml/m ²)	75 +/- 12	78 +/- 15	0.485
LVESVi (ml/m ²)	32 +/- 8	34 +/- 10	0.540
LVEF (%)	57 (49-68)	57 (41-72)	0.892
RVEDV:LVEDV	1.8 +/- 0.4	1.8 +/- 0.5	0.712
Patients with Pulmonary valve intervention <1 year after MRI	13 (36.1%)	13 (40.6%)	0.804
Normally distributed variables are reported as mean +/- standard deviation and non-normally distributed variables are reported as median (range).			

1 **Table 1: Characteristics of patients with repaired Tetralogy of Fallot with normal torsion and reversal of**
2 **basal clockwise rotation.** Reversal of basal clockwise rotation is labeled abnormal torsion. Mann-Whitney U tests
3 were performed for non-normally distributed variables and independent sample t-tests were performed for normally
4 distributed variables. RV= right ventricle, LV= left ventricle, ESVi= end-systolic volume indexed to body surface
5 area, EDVi= indexed end-diastolic volume, EF= ejection fraction.
6

Variable (n=8)	
Patients with shunt prior to initial repair	4 (50%)
Age at MRI (years)	11.9 +/- 8.6 (10.5, 21-27.7)
Time from pulmonary valve intervention to MRI (years)	9.8 +/- 9.1 (6.8, 1.5-27.7)
RVEDVi (ml/m ²)	111 +/- 36
RVESVi (ml/m ²)	55 +/- 21
RVEF (%)	50 +/- 6
LVEDVi (ml/m ²)	69 +/- 12
LVESVi (ml/m ²)	28 +/- 8
LVEF (%)	60 +/- 7
RVEDV:LVEDV	1.7 +/- 0.6
Patients with Pulmonary valve intervention <1 year after MRI	2 (25%)

1 **Table 2: Descriptive characteristics of patients with repaired Tetralogy of Fallot removed from the analysis**
2 **due to inadequate signal to determine torsion based on equilibrated warping.** Normally distributed variables are
3 reported as mean +/- standard deviation and non-normally distributed variables are reported as median (range). RV=
4 right ventricle, LV= left ventricle, ESVi= end-systolic volume indexed to body surface area, EDVi= indexed end-
5 diastolic volume, EF= ejection fraction.
6